

Ultra-Compact accurate wave functions for He-like and Li-like iso-electronic sequences and variational calculus. II. Spin-singlet (excited) and spin-triplet (lowest) states of Helium sequence

A.V. Turbiner,^{*} J.C. Lopez Vieyra,[†] and J.C. del Valle[‡]

Instituto de Ciencias Nucleares, Universidad Nacional Autónoma de México,

A. Postal 70-543 C. P. 04510, Ciudad de México, México.

D.J. Nader[§]

Facultad de Física, Universidad Veracruzana,

A. Postal 70-543 C. P. 91090, Xalapa, Veracruz, México.

Abstract

As a continuation of Part I [1] (Int. Journal of Quantum Chem. 2021; 121: qua.26586), dedicated to the ground state of He-like and Li-like isoelectronic sequences for nuclear charges $Z \leq 20$, a few ultra-compact wave functions in the form of generalized Hylleraas-Kinoshita functions are constructed, which describe the domain of applicability of the Quantum Mechanics of Coulomb Charges (QMCC) for energies (4-5 significant digits (s.d.)) of two excited states of He-like ions: the spin-singlet (first) excited state 2^1S and for lowest spin-triplet 1^3S state. For both states it provides absolute accuracy for energy $\sim 10^{-3}$ a.u., exact values for cusp parameters and also for 6 expectation values the relative accuracy $\sim 10^{-2}$. Bressanini-Reynolds observation about the special form of nodal surface of 2^1S state for Helium is confirmed and extended to ions with $Z > 2$. Critical charges $Z = Z_B$, where ultra-compact trial functions loose their square-integrability, are estimated: $Z_B(1^1S) \approx Z_B(2^1S) \sim 0.905$ and $Z_B(1^3S) \sim 0.902$. For both states the Majorana formula - the energy as the second degree polynomial in Z - provides accurately the 4-5 significant digits for $Z \leq 20$.

^{*} turbiner@nucleares.unam.mx, alexander.turbiner@stonybrook.edu

[†] vieyra@nucleares.unam.mx

[‡] delvalle@correo.nucleares.unam.mx

[§] daniel.nader@correo.nucleares.unam.mx

INTRODUCTION

Search for compact approximation of wave functions is one of interesting open directions in contemporary quantum mechanics. In the case of few-body Coulomb problems it allows to gain understanding of physics of interactions between bodies in small atoms and molecules [2–5] and in particular [6]. Likely, it was the original idea by E.A. Hylleraas when he introduced the so-called “Hylleraas function” for the helium atom [7]. Contrary to the highly complicated variational trial functions composed by thousands of terms, which lead to highly accurate energies, compact wave functions can be easily interpreted. In particular, it is quite valuable if the wave function includes non-linear parameters, which admit a physical meaning of charge screening, their optimal values provide understanding the physics picture of the Coulombic interactions in media. In this sense Mulliken [8] expressed himself in favor of physical intuition or, saying differently, the qualitative physics picture behind contrary to the high accuracy. Needless to say that compact trial functions are specially valuable when they are sufficiently accurate locally (in coordinate space) to be able to reproduce the domain which is free of possible corrections of any type: relativistic, QED, finite mass, etc. For the He-like and Li-like isoelectronic sequences the correction-less domain for the ground state energy was localized in [9]: it was of order of 4 significant digits (s.d.). It is natural to assume this correction-less domain remains unchanged for excited states.

Perhaps, it should be also emphasized that the compact trial functions are not only valuable in order to gain understanding of quantum mechanics of compact few-body systems - bound state - but they are also of interest to the collision community [10]. It turns out that simple but accurate wave functions are very useful as a starting point in the calculation of double ionization cross section by electron or radiation impact. Highly sophisticated wavefunctions with large numbers of terms and parameters are frequently non-practical since they require time-demanding computer codes to evaluate cross sections.

In Part I [1] we introduced (ultra)-compact wave functions for He-like and Li-like isoelectronic sequences in their respective ground states with idea to get a description of the above-mentioned correction-less domain. These ultra-compact wave functions with a few linear and non-linear variational parameters led to accurate variational energies but also provide highly accurate expectation values while satisfying cusp conditions with high accuracy. Furthermore, the non-linear parameters of those wave functions can be systematically

adjusted versus the nuclear charge Z using the quadratic fit in Z for $Z \leq 20$. Moving in Z the relative accuracy in energy is kept fixed: however, it even gets improved for larger nuclear charges. In general, for any of both sequences at $Z \leq 20$ the ground state energy is described by the second degree polynomial in Z - the Majorana formula - with 4-5 significant digits, it corresponds to the correction-less region.

This paper is the second part of the series where we follow the same philosophy of design of (ultra)-compact wave functions for the lowest excited S -states of para- and ortho-Helium, and their respective isoelectronic sequences in the domain of nuclear charges $Z \leq 20$. The structure of this paper is the following: in Section I we discuss the He-like, two-electron sequence, considering the first excited spin-singlet state 2^1S while in Section II the lowest spin-triplet state 1^3S . The results are summarized in Conclusions.

Atomic units are used throughout this paper.

I. SPIN-SINGLET EXCITED STATE 2^1S (PARA-HELIUM SEQUENCE): GENERALIZING HYLLERAAS AND KINOSHITA FUNCTIONS

A. Generalities, exact solution

In general, the orbital function for any spin-singlet state (para-Helium) with zero total angular momentum depends on relative distances only, see e.g. [11]. It is symmetric with respect to permutation of electrons,

$$\Psi(r_1, r_2, r_{12}) = \Psi(r_2, r_1, r_{12}) ,$$

and usually can be represented as

$$\Psi(r_1, r_2, r_{12}) = (1 + P_{12}) \Phi(r_1, r_2, r_{12}) = \Phi(r_1, r_2, r_{12}) + \Phi(r_2, r_1, r_{12}) , \quad (1)$$

where P_{12} is permutation operator ($1 \leftrightarrow 2$).

The orbital function obeys to the reduced Schrödinger equation

$$\hat{H} \Psi(r_1, r_2, r_{12}) = E \Psi(r_1, r_2, r_{12}) , \quad (2)$$

where $\hat{H} = \hat{H}(r_1, r_2, r_{12})$,

$$\begin{aligned} \hat{H} = & -\frac{1}{2} \left[\frac{\partial^2}{\partial r_1^2} + \frac{\partial^2}{\partial r_2^2} + 2 \frac{\partial^2}{\partial r_{12}^2} + \frac{2}{r_1} \frac{\partial}{\partial r_1} + \frac{2}{r_2} \frac{\partial}{\partial r_2} + \frac{4}{r_{12}} \frac{\partial}{\partial r_{12}} \right. \\ & + \left(\frac{r_1^2 - r_2^2 + r_{12}^2}{r_1 r_{12}} \right) \frac{\partial^2}{\partial r_1 \partial r_{12}} + \left(\frac{r_2^2 - r_1^2 + r_{12}^2}{r_2 r_{12}} \right) \frac{\partial^2}{\partial r_2 \partial r_{12}} \Big] \\ & + \left[\frac{-Z}{r_1} + \frac{-Z}{r_2} + \frac{1}{r_{12}} \right] , \end{aligned} \quad (3)$$

see in [12] the Eq.(5), is the so-called *radial* 3-body Schrödinger Hamiltonian [11]. Here, r_1 and r_2 are the electron distances from the nucleus of charge Z , while r_{12} is interelectronic distance.

From (3) it is easy to obtain the first terms of the so-called Fock expansion for orbital function of arbitrary spin-singlet, permutationally-symmetric ($r_1 \leftrightarrow r_2$) state

$$\Psi = 1 - C_{Z,e}(r_1 + r_2) + C_{e,e} r_{12} + \dots , \quad (4)$$

where the coefficients

$$C_{Z,e} = Z \quad , \quad C_{e,e} = \frac{1}{2} , \quad (5)$$

are called the *cusp* parameters. They have a meaning of residues in Coulomb singularities of the potential.

Making in (2)-(3) the scale transformation,

$$r \rightarrow u = Zr ,$$

one can see that the kinetic energy operator in \hat{H} remains unchanged up to the multiplicative factor Z^2 , while the potential energy and the spectral parameter E are changed. We arrive at the radial Schrödinger like equation

$$\hat{H} \Psi(u_1, u_2, u_{12}) = \varepsilon \Psi(u_1, u_2, u_{12}) , \quad (6)$$

where

$$\begin{aligned} \hat{H} = & -\frac{1}{2} \left[\frac{\partial^2}{\partial u_1^2} + \frac{\partial^2}{\partial u_2^2} + 2 \frac{\partial^2}{\partial u_{12}^2} + \frac{2}{u_1} \frac{\partial}{\partial u_1} + \frac{2}{u_2} \frac{\partial}{\partial u_2} + \frac{4}{u_{12}} \frac{\partial}{\partial u_{12}} \right. \\ & + \left(\frac{u_1^2 - u_2^2 + u_{12}^2}{u_1 u_{12}} \right) \frac{\partial^2}{\partial u_1 \partial u_{12}} + \left(\frac{u_2^2 - u_1^2 + u_{12}^2}{u_2 u_{12}} \right) \frac{\partial^2}{\partial u_2 \partial u_{12}} \Big] \\ & + \left[-\frac{1}{u_1} - \frac{1}{u_2} + \frac{1}{Z} \frac{1}{u_{12}} \right], \quad \varepsilon = \frac{E}{Z^2}, \end{aligned} \quad (7)$$

plays the role of the Hamiltonian, it describes two hydrogen atoms with interelectron repulsion and unusually-written kinetic energy.

At $Z \rightarrow \infty$ the spectral problem (6) with the Hamiltonian (7) corresponds to two non-interacting hydrogen atoms, u_{12} dependence disappears and variables u_1, u_2 are separated. As a realization of permutation symmetry ($1 \leftrightarrow 2$) the exact eigenfunctions appear as the sum of symmetrized products of two Coulomb orbitals. The ground state ($1s1s\ 1^1S$) can be presented as

$$\Psi_0 = \frac{1}{2}(1 + P_{12}) e^{-\alpha u_1 - \beta u_2} \sim (1s_1 1s_2) + (1s_2 1s_1), \quad (8)$$

when $\alpha = \beta = 1$, the ground state energy $E_0 = -Z^2$ is twice of the ground state of the hydrogen atom. In turn, the first excited state ($1s2s\ 2^1S$) is made from symmetrized ($2s_1 1s_2$) hydrogenic Coulomb orbitals,

$$\Psi_1 = \frac{1}{2}(1 + P_{12}) (1 - a u_1) e^{-\alpha u_1 - \beta u_2} \sim (2s_1 1s_2) + (1s_1 2s_2), \quad (9)$$

where $a = 1/2, \alpha = 1/2, \beta = 1$ with eigenvalue

$$E_1 = -\frac{5Z^2}{8}, \quad (10)$$

which is evidently orthogonal to the ground state (8). The nodal surface, where $\Psi_1 = 0$, is symmetric $u_1 \leftrightarrow u_2$, it starts at the point $u_1 = u_2 = 2$ and then it goes to the end-point $u_1(u_2) = 0$, the value of $u_2(u_1) = 2.556929$.

Needless to say that the function Ψ_1 (9) can be used as trial function for any integer $Z = 2, 3, \dots$ if the orthogonality condition to the ground state, taken for instance in the form (8), is imposed. It fixes the parameter a in terms of α, β , those eventually are used as variational parameters. It resembles the function used by Stillinger and Stillinger for the ground state ($1s1s\ 1^1S$) of He-like sequence [13].

B. Compact trial functions

Natural generalization of (9), where interelectron distance is involved explicitly, emerging from interpolation between Hylleraas-type ($b = 0$) [7] and Kinoshita-type ($a = 0, \gamma = 0$) [14] functions has the form

$$\Psi_{HK} = \frac{1}{2}(1 + P_{12})(1 - aZr_1 + br_{12}) e^{-\alpha Zr_1 - \beta Zr_2 + \gamma r_{12}} , \quad (11)$$

cf.(1), which can be further generalized to

$$\Psi_G = \frac{1}{2}(1 + P_{12})(1 - aZ\hat{r}_1 + br_{12}) e^{-\alpha Z\hat{r}_1 - \beta Zr_2 + \gamma \hat{r}_{12}} . \quad (12)$$

In the latter function the effects of screening, which are different for small and large distances, are taken into account by replacing $r_1 \rightarrow \hat{r}_1$ and $r_{12} \rightarrow \hat{r}_{12}$ in the exponential, see below. From the physics viewpoint the first terms in exponential of Ψ_{HK}, Ψ_G reflect the fact that the second electron is situated (in average) closer to the nucleus than the first one, $\alpha > \beta$ (it is the so-called clusterization effect). Hence, the interaction of the 2nd electron with nucleus can be considered as non-screened, $\beta \sim 1$, unlike the 1st one, for which the interaction with nucleus is screened by the presence of the second electron. Therefore, for the 1st electron the screening should be taken into account explicitly, for example, like

$$\alpha r_1 \rightarrow \alpha \hat{r}_1 \equiv \alpha r_1 \frac{1 + cr_1}{1 + dr_1} ,$$

see [6]. In a similar way the screening of the Coulomb repulsion between electrons due to presence of nucleus somehow in between of them should be turned on, for example, in the form,

$$\gamma r_{12} \rightarrow \gamma \hat{r}_{12} \equiv \gamma r_{12} \frac{1 + c_{12}r_{12}}{1 + d_{12}r_{12}} .$$

It depends on interelectronic distance.

In order to perform concrete calculations for the excited state ($1s2s\ 2^1S$) the orthogonality condition $(\Psi^{(ground\ state)}, \Psi_1) = 0$ to the ground state should be imposed. It allows to fix one of the parameters (we choose the parameter a) and eventually the trial functions (11), (12) become 4- and 8-parametric, respectively. The ground state function was taken from Part I [1] in two forms, as the Hylleraas-Kinoshita function $\Psi_{HK}^{(ground)}$, see Eq.(17) in Part I, and the seven-parametric generalized Hylleraas-Kinoshita function $\Psi_F^{(ground)}$, see Eq.(23)

in Part I, with fitted parameters Eq.(28). Then the variational calculation was carried out. The results of calculations are presented in Table I for $Z = 3/2, 2, 10, 20$. Surprising observation is that the accurate variational energies are compatible with $b = 0$ for both trial functions (11), (12), independently on Z , if the accuracy of 4-5 s.d. is considered. It reduces effectively a number of variational parameters. Inside of this accuracy we did not observe the dependence on the variational results on the ground state function chosen. Essentially, the parameter (Za) depends on Z linearly, see below.

Table I: Variational energy of first spin-singlet excited state E_1 of the helium-like atom at $Z = 3/2, 2, 10, 20$ calculated with Ψ_{HK} (11) and Ψ_G (12). Orthogonality constraint imposed with respect to the Hylleraas-Kinoshita function for the ground state, see [1], Eq.(17) and Ψ_F , see [1] Eq.(23) with parameters (28), respectively. Electron-nuclear cusp $C_{Z,e}$ and electron-electron cusp $C_{e,e}$ shown (ratio of expectation values is on first row, while second row results found via the expansion (4) of Ψ_{HK}), on the third row the cusp parameters fixed to be exact and the results of constrained minimization of the variational energy for Ψ_G (12) shown.

Z	E^{HK}	E^G	$C_{Z,e}$	$C_{e,e}$	E_{ref}	$E_M^{(2S)}$
3/2	-1.1654		1.4963	0.0199	-	-1.16755
			1.1353	0.0199		
		-1.1663	1.5	0.5		
2	-2.1438		1.9864	0.0363	-2.1460 [†]	-2.14552
			1.6485	0.0363		
		-2.1460	2.0	0.5		
10	-60.2882		9.9322	0.0956	-60.2953*	-60.2931
			9.6886	0.0956		
		-60.2946	10.0	0.5		
20	-245.4709		19.9265	0.1032	-245.4776*	-245.478
			19.7000	0.1032		
		-245.4770	20.0	0.5		

[†] non-rounded results: $E = -2.145\,974\,021$ [15], $E = -2.145\,974\,046\,054$ [16], $E = -2.145\,974\,046\,054\,419(6)$ [17]; all three coincide in 8 s.d.

* calculated using the code provided in [15]

In general, the variational parameters in Ψ_G (12) leading to the minimal energy for the spin-singlet excited state E_1 of the helium-like atom at $Z = 3/2, 2, 10, 20$ have a smooth behavior as a function of the nuclear charge Z . In particular, the parameters of the constrained minimization which is required to reproduce exact cusp parameters $C_{Z,e} = Z$ and

Table II: Expectation values for the excited state ($1s2s\ 2^1S$) using the function Ψ_G , constrained (first row) and unconstrained (second row). Results by Accad-Pekeris-Schiff [28], by Braun-Schweizer-Herold [29] and Liverts-Barnea [15] ^(*) included for comparison. Electron-nuclear cusp $C_{Z,e}$ and electron-electron cusp $C_{e,e}$ found via the expansion (4) of Ψ_G , i.e. $C_{Z,e} = ((\alpha + \beta)Z + a)/2$, $C_{e,e} = b + \gamma$.

Z	E	$C_{Z,e}$	$C_{e,e}$	$\langle\delta(\mathbf{r}_1)\rangle$	$\langle\delta(\mathbf{r}_{12})\rangle$	$\langle r_1 \rangle$	$\langle r_1^2 \rangle$	$\langle r_{12} \rangle$	$\langle r_{12}^2 \rangle$	source
3/2	-1.16626	1.5	0.5	0.5432	0.00154	5.16634	51.67048	9.40825	103.51640	
		1.59279	0.58884	0.5439	0.00135	5.09344	49.77424	9.26241	99.72620	
2	-2.14600	2.0	0.5	1.3195	0.01358	2.88920	15.34402	5.10698	30.7994	
		2.05887	0.53947	1.3079	0.00887	2.97208	16.08416	5.26699	32.27204	
				1.3095	0.00865	2.97306	16.0891	5.26969	32.302	[28]
				1.3094	0.00866	2.97321		5.26959		[15]
						2.97318			32.18126	[29]
10	-60.29456	10.0	0.5	175.1837	5.87751	0.40185	0.26477	0.67128	0.53092	
		9.94772	0.41940	174.6227	5.82404	0.40297	0.26626	0.67341	0.53392	
				174.8737	5.74	0.40289	0.26584	0.67337	0.53338	[28]
				174.8733	5.72932	0.40289		0.67337		[15]
20	-245.47700	20.0	0.5	1417.3854	54.86331	0.19381	0.26477	0.32131	0.12186	
		19.87555	0.40990	1412.6008	54.29124	0.19413	0.06103	0.32190	0.12224	
				1415.0882	53.88928	0.19416		0.32202		[15]

* calculated using the code provided in [15]

$C_{e,e} = 1/2$, can be fitted for $2 \leq Z \leq 20$,

$$\begin{aligned}
Za &= -0.297218 + 0.505737Z - 0.0001968Z^2, \\
b &= 0, \\
c_{12} &= 0.0405438 - 0.032151Z + 0.00031Z^2, \\
d_{12} &= 0.24351 + 0.111263Z + 0.001843Z^2, \\
\alpha &= 0.358158/(Z + 0.2528) + 0.489224 + 0.000358(Z + 0.2528), \\
\beta &= 2 - a - \alpha, \\
\gamma &= 1/2, \\
c &= -0.146884 + 0.162799Z + 0.000512Z^2, \\
d &= 0.123749 + 0.164107Z + 0.0005Z^2.
\end{aligned} \tag{13}$$

The parameter a , given by fit, guarantees approximate orthogonality of Ψ_G to ground state Ψ_F defined in Part I [1]. With above fitted parameters the expectation values for energy E

which coincide with those presented in Table I. It can be shown that the Majorana formula holds for this state

$$E_M^{(2^1S)} = -\frac{5Z^2}{8} + 0.231547Z - 0.108618. \quad (14)$$

It provides accuracy 4 s.d. for $2 \leq Z \leq 20$, see Table I, in a similar way as for the ground state [1].

Six expectation values for the state $(1s2s\,2^1S)$ calculated using the function Ψ_G with unconstrained (free) variational parameters and with variational parameters constrained to reproduce exact cusp values are shown in Table II. There exists an agreement with results by Accad-Pekeris-Schiff [28], Braun-Schweizer-Herold [29] and [15], wherever possible, in 2-3-4 s.d.

C. Nodal surface

Separate issue of the study is related with form of the nodal surface, where $\Psi_1(r_1, r_2, r_{12}) = 0$, for the state $(1s2s\,2^1S)$. This nodal surface divides the coordinate space into two subspaces. Usually, the localization of nodal surface is a difficult task, since in its vicinity the wavefunction is small, which can be smaller than accuracy of any approximate method used. It is worth noting that accurate localization of the nodal surfaces is crucial for employing Monte-Carlo technique for the excited states.

In [16] it was conjectured that for $Z = 2$ the nodal surface for the state $(1s2s\,2^1S)$ has a very weak dependence on the angle between vectors $\mathbf{r}_{1,2}$. At $Z = \infty$ the known exact solution (9) confirms trivially its validity. Taking functions Ψ_{HK}, Ψ_G the conjecture is checked for several $Z \in [2, 20]$, Figs. 1 - 3. One can see that for both trial functions the nodal line, which lies in the first quadrant of (u_1, u_2) plane, in fact, it has almost no dependence on angle $\widehat{(\mathbf{r}_1, \mathbf{r}_2)}$ inside of the accuracy of variational method we used, it is defined by the thickness (!) of the drawing lines presented in Figs. 1 - 3. Nodal lines for different Z look similar with rather weak dependence on Z . Hence, the conjecture by Bressanini and Reynolds [16] holds for nuclear charges Z other than $Z = 2$.

Figure 1: Nodal line for the state $(1s2s\ 2^1S)$ for $Z = \infty$ and for $Z = 2$ for Ψ_{HK} (11), Ψ_G (12) and comparison with nodal line, marked by Ψ_S , found in [16].

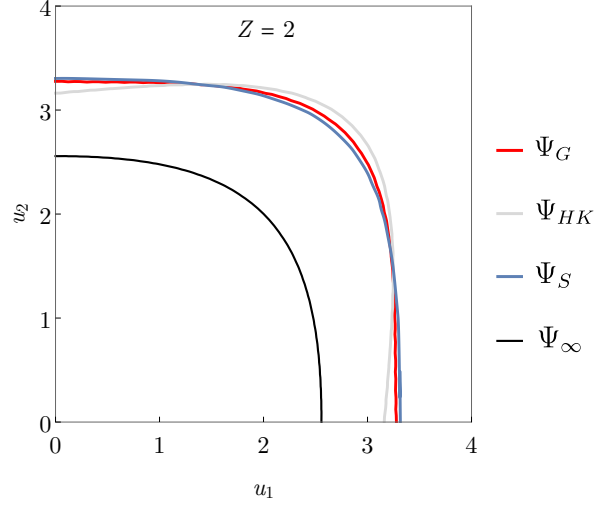
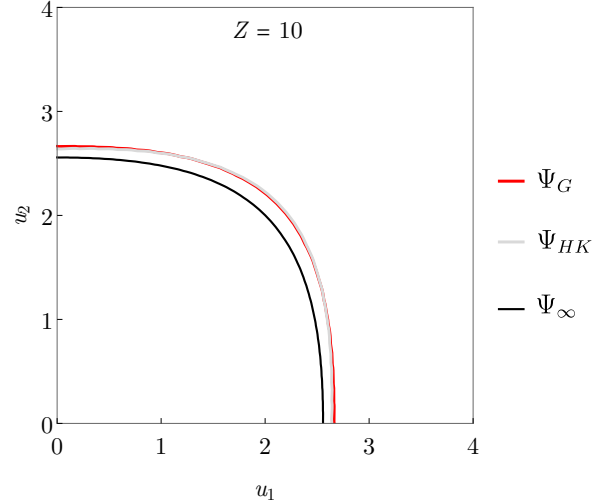


Figure 2: Nodal line for the state $(1s2s\ 2^1S)$ for $Z = \infty$ and for $Z = 10$ for Ψ_{HK} (11), Ψ_G (12).



D. Square-integrability of compact functions

It is evident that for $Z > 1$ keeping the position of one electron fixed the wavefunction decays exponentially at large values of the position of another electron, see for illustration Fig.4. It corresponds to the interaction of hydrogen-like ion (Ze) with electron. It can be explicitly seen if we take one of terms in the representation (1) for the wavefunction,

$$\Phi_1|_{r_2(r_1)fixed} \rightarrow \exp\{-A_{1,2} r_1(r_2)\} \text{ at } r_1(r_2) \rightarrow \infty. \quad (15)$$

Figure 3: Nodal line for the state $(1s2s\ 2^1S)$ for $Z = \infty$ and for $Z = 20$ for Ψ_{HK} (11), Ψ_G (12).

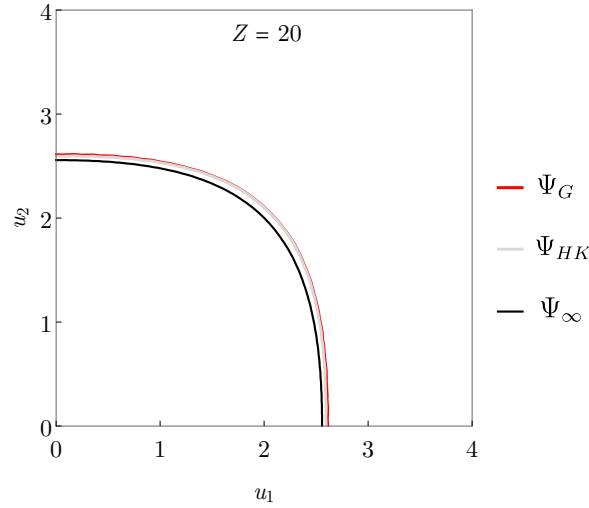
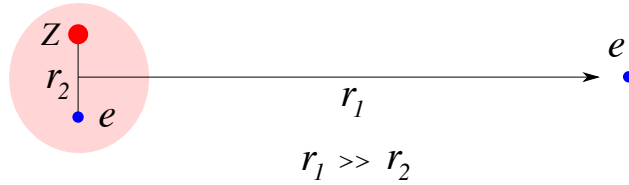


Figure 4: Configuration which corresponds to the interaction of hydrogen-like ion (Ze) with electron.



In particular, at $Z \rightarrow \infty$ for the exact ground state function (8) in the case of the first term it gives

$$A_1^{(0)} = Z, \quad A_2^{(0)} = Z, \quad (16)$$

while for the first excited state ($1s2s$) the exact wavefunction (9) leads to,

$$A_1^{(1)} = \frac{1}{2}Z, \quad A_2^{(1)} = Z. \quad (17)$$

Straightforwardly, it implies that at $Z = Z_B^{(0,1)} = 0$ square-integrability of (8),(9) is lost, which is well beyond of the domain where the exact solutions make sense.

Let us take the first term of $\Psi_G(r_1, r_2, r_{12})$ (12) for the excited state ($1s2s\ 2^1S$), which is the most accurate compact wave function we constructed. It is easy to find that

$$A_1^{ES} = \alpha Z \frac{c}{d} - \gamma \frac{c_{12}}{d_{12}}, \quad A_2^{ES} = \beta Z - \gamma \frac{c_{12}}{d_{12}}. \quad (18)$$

Similar formulas occurs for the second term. In concrete calculations one can find that for

all studied $Z \leq 20$

$$A_1^{ES} < A_2^{ES} ,$$

it signals the appearance of clusterization effect: the electron 2 is closer to the nuclei than the electron 1. The rate of convergence of variational integrals is defined by A_1^{ES} .

In a similar way the analysis can be performed for the ground state, see Part I, Eq.(23), which leads to

$$A_1^{GS} = \alpha Z - \gamma \frac{c_{12}}{d_{12}} , \quad A_2^{GS} = \beta Z - \gamma \frac{c_{12}}{d_{12}} , \quad (19)$$

and for all studied Z

$$A_1^{GS} > A_2^{GS} .$$

The rate of convergence of variational integrals is defined by A_2^{GS} .

In Fig.5 the dependence on A_2^{GS}, A_1^{ES} *versus* Z , found numerically, is shown. Systematically, $A_2^{GS} > A_1^{ES}$. With high accuracy both curves self-intersect and simultaneously vanish(!) at $Z = Z_B \sim 0.905$, which corresponds to the so-called second critical charge Z_B , see [9, 18] and references therein, where both functions loose their square-integrability. It is an indication that at $Z = Z_B$ there is the second-order branch point in energy in Z -plane with a meaning of crossing of the ground state energy with the first excited state energy as was predicted in [18]. It leads to appearance of the Puiseux expansion of the energy at $Z = Z_B$ [19]. It is natural to assume that namely this branch point defines the radius of convergence of $1/Z$ expansion for both states. With high accuracy both A_2^{GS}, A_1^{ES} are interpolated by

$$b_{1/2}(Z - Z_B)^{1/2} + b_1(Z - Z_B)$$

where $b_{1/2}$ is small, while $b_1 = 1$ for A_2^{GS} and $b_1 = 1/2$ for A_1^{ES} in agreement with shell model, see (16), (17).

It is interesting that for $Z = 1$ both A_2^{GS}, A_1^{ES} take positive values, $0.117222(a.u.)^{-1}$ and $0.047625(a.u.)^{-1}$, respectively, which indicate to square-integrability of functions $\Psi_{G,F}$, respectively ¹. Corresponding energies are $E^{GS} = -0.52725$ a.u. , which is very close to the exact value -0.52775 a.u. (they differ in the 4th d.d.), for the ground state of negative ion of hydrogen, H^- , while $E^{ES} = -0.49998$ a.u. for the 1st excited state, respectively. For the latter state the energy is very close to threshold $E_{threshold} = -0.5$ a.u. being above of it: it

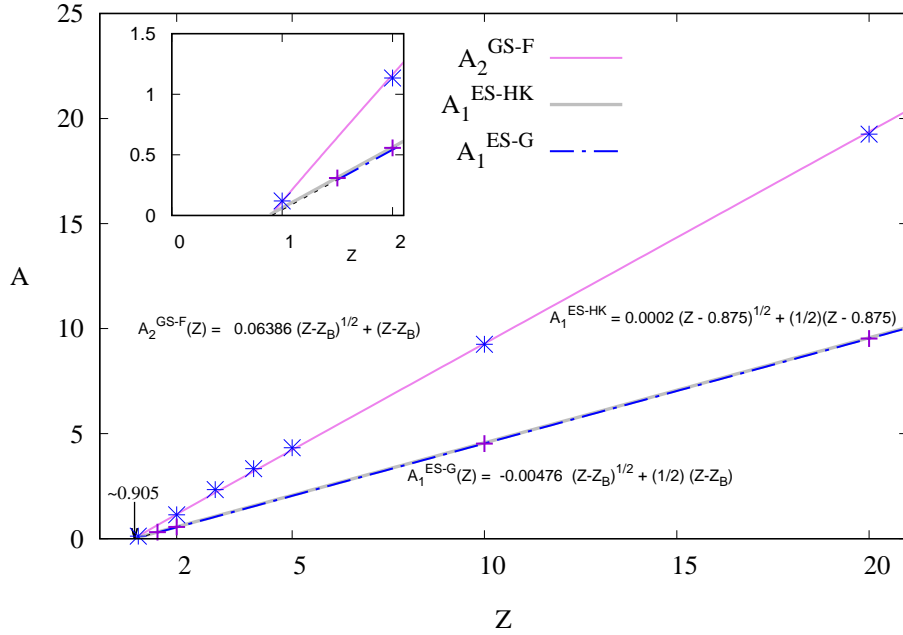
¹ At $Z = 1$ the potential of interaction of neutral core (hydrogen atom) with distant electron is attractive, it behaves like $-1/r^4$ and generates van-der-Waals minimum, for discussion see e.g. [20]

is the level embedded to continuum within the accuracy which the function Ψ_G provides. The interesting question what would happen if more accurate function than Ψ_G is taken as the trial function, will this level become the bound state with energy below threshold - it is not clear to the present authors, it might be a subject of separate study.

It is well known that there exists the critical charge $Z_{cr} = 0.911028\dots$, for which the exact ground state energy $E^{GS} = -0.41496\dots$ a.u., calculated variationally in [21] and confirmed in Lagrange Mesh Method in [22] with high accuracy, coincides with corresponding threshold of the continuous spectra. In both calculations [21] and [22] the ground state function at $Z = Z_{cr}$ is square-integrable in agreement with the general theory, see e.g. [23]. In present calculation both the ground state function Ψ_G , see Part I, and the spin-singlet first excited state Ψ_F function remain square-integrable, since both A_2^{GS}, A_1^{ES} take positive values at $Z = Z_{cr}$. The excited state at $Z = Z_{cr}$ continues to correspond to the level embedded to continuum. In both states the system is of finite size. In further decrease of $Z < Z_{cr}$ both wavefunctions remain square-integrable, $A_2^{GS}, A_1^{ES} > 0$ - the size of the system is finite for both states in agreement with prediction by Stillinger-Stillinger [13], but contrary to that was stated in [24]. At $Z = Z_B$ the square-integrability of both functions is lost simultaneously and the size of the system gets infinite for both states.

Figure 5: He-like sequence, $(1s2s\ 2^1S)$ and $(1s1s\ 1^1S)$ states:

- (a) the parameter $A_1^{(ES)}$ vs Z for the functions Ψ_{HK} (11) and Ψ_G (12) shown (lower curves), which “measures” their square-integrability, see text. For $Z \leq 3/2$ the dot-dashed part of the curve and dotted curve are the extrapolation, see embedded subfigure,
(b) for the ground state $(1s1s\ 1^1S)$ the parameter $A_2^{(GS)}$ vs Z for the function Ψ_F , see Part I, Eq.(23), is shown (upper curve), it almost coincides with curve $A_2^{(GS-HK)}$ (not shown) with $Z_B^{(GS-HK)} \sim 0.887$.
(c) With high accuracy curves $A_1^{(ES-G)}$ and $A_2^{(GS-F)}$ intersect at $Z = Z_B^{(ES-G)} = Z_B^{(GS-F)} \sim 0.905$, where square-integrability is lost for both states simultaneously. Dash-dotted curve corresponds to Hylleraas-Kinoshita function (11) with $Z_B^{(ES-HK)} \sim 0.875$.



II. SPIN-TRIPLET STATE 1^3S (ORTHO-HELIUM SEQUENCE): GENERALIZING HYLLERAAS FUNCTION

A. Generalities, exact solution

Orbital functions for spin-triplet state at zero total angular momentum depend on relative distances (r_1, r_2, r_{12}) between bodies and they are antisymmetric,

$$\Psi^{(-)}(r_1, r_2, r_{12}) = -\Psi^{(-)}(r_2, r_1, r_{12}) ,$$

hence, it might be written as

$$\Psi^{(-)}(r_1, r_2, r_{12}) = (1 - P_{12}) \phi(r_1, r_2, r_{12}) = \phi(r_1, r_2, r_{12}) - \phi(r_2, r_1, r_{12}) . \quad (20)$$

It implies the existence of nodal surface

$$r_1 = r_2 .$$

It suggests to employ the representation

$$\Psi^{(-)}(r_1, r_2, r_{12}) = (r_1 - r_2) \psi(r_1, r_2, r_{12}) ,$$

where ψ is symmetric, $\psi(r_1, r_2, r_{12}) = \psi(r_2, r_1, r_{12})$. Permutationally-symmetric function ψ is the eigenfunction of the gauge rotated Hamiltonian,

$$\begin{aligned} \hat{\mathcal{H}} = (r_1 - r_2)^{-1} \hat{H} (r_1 - r_2) = \\ -\frac{1}{2} \left[\frac{\partial^2}{\partial r_1^2} + \frac{\partial^2}{\partial r_2^2} + 2 \frac{\partial^2}{\partial r_{12}^2} + 2 \left(\frac{1}{r_1 - r_2} + \frac{1}{r_1} \right) \frac{\partial}{\partial r_1} + 2 \left(\frac{1}{r_2 - r_1} + \frac{1}{r_2} \right) \frac{\partial}{\partial r_2} \right. \\ \left. + \left[\frac{r_1^2 + 6r_1 r_2 + r_2^2 - r_{12}^2}{r_1 r_2 r_{12}} \right] \frac{\partial}{\partial r_{12}} + \left[\frac{r_1^2 - r_2^2 + r_{12}^2}{r_1 r_{12}} \right] \frac{\partial^2}{\partial r_1 \partial r_{12}} + \left[\frac{r_2^2 - r_1^2 + r_{12}^2}{r_2 r_{12}} \right] \frac{\partial^2}{\partial r_2 \partial r_{12}} \right] \\ + \left[\frac{-Z}{r_1} + \frac{-Z}{r_2} + \frac{\delta}{r_{12}} + \frac{1}{r_1 r_2} \right] , \end{aligned} \quad (21)$$

where \hat{H} is the original (reduced) Hamiltonian acting in (r_1, r_2, r_{12}) space, see [12] and [1]; here the parameter $\delta = 1$ - it is introduced for the sake of convenience. Eventually, the eigenvalue problem

$$\hat{\mathcal{H}}\psi = E\psi , \quad \psi(r_1, r_2, r_{12}) \in L^2(\mathbf{R}_+^3) , \quad (22)$$

occurs where the condition $\psi(0, 0, 0) = 0$ should be imposed.

At $Z \rightarrow \infty$ (equivalently, $\delta = 0$) for the lowest energy spin-triplet state ($1s2s\ 1^3S$), there exists the exact eigenfunction in the form of anti-symmetrized product of ($2s1s$) orbitals,

$$\Psi_0^{(-)} = \frac{1}{2}(1 - P_{12})(1 - aZr_1) e^{-\alpha Zr_1 - \beta Zr_2} \sim (2s_1 1s_2) - (1s_1 2s_2) , \quad (23)$$

where $a = 1/2, \alpha = 1/2, \beta = 1$; they are related as

$$a = -\alpha + \beta , \quad (24)$$

with eigenvalue

$$E_0 = -\frac{5Z^2}{8}, \quad (25)$$

cf. (9), (10).

Making the analysis of the Schrödinger equation for the Hamiltonian (21) it can be shown that at small distances a solution admits the analogue of the Fock expansion for the ground state

$$\begin{aligned} \Psi(r_1, r_2, r_{12}) = & (r_1 - r_2) \\ & (K + (r_1 + r_2) + D_0 r_{12} - A(r_1^2 + r_2^2) - B r_1 r_2 + C(r_1 + r_2)r_{12} + D r_{12}^2 + \dots) \end{aligned} \quad (26)$$

with

$$A = \frac{2Z}{3}, \quad B = \frac{5Z}{3}, \quad C = \frac{\delta}{4}, \quad K = D_0 = D = 0,$$

thus, the constant term in expansion of the second factor is absent as well as the terms r_{12}, r_{12}^2 . We call the cusp parameters the following expressions

$$C_{Z,e}^{(1)} = (-A + B) = Z, \quad C_{Z,e}^{(2)} = (4A - B) = Z, \quad C_{e,e} = 4C = \delta (= 1), \quad (27)$$

having the meaning of residues at Coulomb singularities of the potential. Alternatively, the electron-nuclear cusps can be calculated through the ratio of expectation values

$$\tilde{C}_{Z,e}^{(i)} \equiv -\frac{\langle \delta(\mathbf{r}_i) \frac{\partial}{\partial r_i} \rangle}{\langle \delta(\mathbf{r}_i) \rangle}, \quad i = 1, 2, \quad (28)$$

see [25] and also [1]. For the exact eigenfunction $\tilde{C}_{Z,e}^{(1,2)} = Z$.

B. Compact trial functions for spin-triplet state

A straightforward way to construct trial functions for spin triplet state is by making a generalization of the procedure used for spin singlet state

$$\Psi_a^{(-)} = (1 - P_{12}) \Psi_0(r_1, r_2, r_{12}) = \Psi_0(r_1, r_2, r_{12}) - \Psi_0(r_2, r_1, r_{12}). \quad (29)$$

Imposing the condition that $\Psi_a^{(-)}$ should reproduce at $Z \rightarrow \infty$ the exact solution (23), one can construct the negative parity analogue of Hylleraas function,

$$\Psi_H^{(-)} = \frac{1}{2}(1 - P_{12})(1 - aZr_1)e^{-\alpha Zr_1 - \beta Zr_2 + \gamma r_{12}}, \quad (30)$$

This function is characterized by four free parameters with one constraint (24), $a = -\alpha + \beta$, due to boundary condition for (22), or equivalently, $K = 0$ in (26). Extra conditions $D_0 = D = 0$ from (26) - the absence of the terms r_{12}, r_{12}^2 - are fulfilled automatically. Cusp parameters are easily found,

$$C_{Z,e}^{(1)} = \beta Z \quad , \quad C_{Z,e}^{(2)} = 2\alpha Z \quad , \quad C_{e,e} = \gamma . \quad (31)$$

The variational calculations can be carried out analytically, the results are presented in Table II.

There is another trial function, which takes into account the effect of screening of electron-electron interaction due to presence of charge Z and which seems essential, it appears as the generalization of the Hylleraas function (30),

$$\Psi_F^{(-)} = \frac{1}{2} (1 - P_{12}) \left[(1 + (\alpha - \beta) Z r_1) e^{-\alpha Z r_1 - \beta Z r_2 + \gamma r_{12} \frac{(1+cr_{12})}{(1+dr_{12})}} \right] , \quad (32)$$

where $\alpha, \beta, \gamma, c, d$ are 5 free parameters; $K = 0$ and conditions $D_0 = D = 0$ from (26) in the expansion of $\Psi_F^{(-)}$ at small distances continue to be fulfilled. The cusp parameters are the same as in (31). The results of variational calculations are presented in Table II.

The function (32) can be further generalized to

$$\Psi_G^{(-)} = \frac{1}{2} (1 - P_{12}) \left[(1 + (\alpha - \beta) Z r_1 - a(r_1 + r_2)) e^{-\alpha Z r_1 \frac{(1+c_1 r_1)}{(1+d_1 r_1)} - \beta Z r_2 + \gamma r_{12} \frac{(1+c_{12} r_{12})}{(1+d_{12} r_{12})}} \right] , \quad (33)$$

where the screening of interaction of ($2s$) electron, marked by 1, with charge Z is taken into account as well as the screening of interelectron interaction. This function is going to be used in final calculations, see Table II. This function contains 8 free parameters; the cusp parameters are,

$$\begin{aligned} C_{Z,e}^{(1)} &= \frac{((\alpha - \beta) \beta Z - (\alpha + \beta) a) Z + 2 \tilde{\alpha} \delta_1 (a + \beta Z)}{(\alpha - \beta) Z - 2a + 2 \tilde{\alpha} \delta_1} , \\ C_{Z,e}^{(2)} &= 2 \frac{((\alpha - \beta) \alpha Z - (\alpha + \beta) a) Z + 2 \tilde{\alpha} \delta_1 (a + \beta Z) + 3 d_1 \tilde{\alpha} \delta_1}{(\alpha - \beta) Z - 2a + 2 \tilde{\alpha} \delta_1} , \\ C_{e,e} &= \gamma , \end{aligned} \quad (34)$$

where $\delta_1 = c_1 - d_1$ and $\tilde{\alpha} = \alpha/(\alpha - \beta)$. Further generalization does not look necessary. It does lead to improvement of energy E_{var} obtained with $\Psi_G^{(-)}$ (see Table II, column 5) in 5th decimal digit, which is beyond the scope of the present paper.

Imposing three constraints on parameters in (33), see (34), in particular, choosing $\gamma = 1/4$, one can reproduce cusp values (27) exactly. The energies obtained with such constrained parameters (after making minimization with respect to five free parameters) for the function (33) are presented in Table II, column 4. The remaining free parameters can be easily fitted by the following functions

$$\begin{aligned}
\alpha Z &= -0.16755 + 0.37339Z + 0.00762Z^2, \\
\beta Z &= 0.005394 + 1.00163Z - 0.000086Z^2, \\
c_{12} &= -0.06847 + 0.07471Z - 0.00537Z^2, \\
d_{12} &= -0.07878 + 0.47309Z - 0.02018Z^2, \\
c_1 &= 1.11157 + 0.43103Z - 0.02155Z^2.
\end{aligned} \tag{35}$$

These fitted parameters allow us to obtain expectation values for energies for any value $Z \leq 20$ with sufficiently high accuracy, see Table II. In particular, for $Z = 15$ the fitted parameters (31) lead to the expectation value for energy $E = -137.825$ a.u., while the Majorana formula (36), see below, gives $E = -137.854$ a.u.

Interestingly, for $Z = 2$ all trial functions used allow us to reproduce 4 s.d. in energy, while $\Psi_G^{(-)}$ (unconstrained) result is in agreement with benchmark results [26] in 5 s.d. as well as [28] and [29]. Note that for $Z = 10, 20$ functions $\Psi_F^{(-)}$ and $\Psi_G^{(-)}$ in spite of their simplicity lead to the lower energies in comparison with old benchmark calculations [27].

Table III: Comparison of the lowest energy spin-triplet state ($1s2s\ 1^3S$) for Helium-like atomic ions at $Z = 3/2, 2, 10, 20$ calculated variationally using the Hylleraas function $\Psi_H^{(-)}$ (30), with the function $\Psi_F^{(-)}$ (32) and with function $\Psi_G^{(-)}$ (33) (constrained, where it is imposed: cusp values $C_{Z,e}^{(1)} = C_{Z,e}^{(2)} = Z$, $C_{e,e} = 1$ reproduced *exactly*), and (un-constrained, where all 8 parameters free). The energy E_{var} in a.u., the nuclear-electron cusps $C_{Z,e}$ and electron-electron cusp $C_{e,e}$ shown. Last column shows energies from [26]^a, [27]^b

Z	$\Psi_H^{(-)}$			$\Psi_F^{(-)}$			$\Psi_G^{(-)}$ (constrained)			$\Psi_G^{(-)}$ (un-constrained)			E_{refs}	E_{Majorana}
	E_{var}	$C_{Z,e}^{(1)}/C_{Z,e}^{(2)}$	$C_{e,e}/4$	E_{var}	$C_{Z,e}^{(1)}/C_{Z,e}^{(2)}$	$C_{e,e}/4$	E_{var}	$C_{Z,e}^{(1)}/C_{Z,e}^{(2)}$	$C_{e,e}/4$	E_{var}	$C_{Z,e}^{(1)}/C_{Z,e}^{(2)}$	$C_{e,e}/4$		
3/2	-1.1773	1.504	0.026	-1.1774	1.504	0.25	-1.1774	1.500	0.250	-1.17758	1.517	0.206		-1.17482
		0.803			0.802			1.500			0.982			
2	-2.1749	2.007	0.035	-2.1750	2.006	0.25	-2.1750	2.000	0.250	-2.17515	2.019	0.214	-2.17523 ^a	-2.1745
		1.351			1.349			2.000			1.482			
10	-60.6681	10.013	0.053	-60.6684	10.011	0.250	-60.66847	10.000	0.250	-60.66852	10.036	0.225	-60.66835 ^b	-60.6694
		9.415			9.411			10.000			9.538			
20	-246.2886	20.014	0.054	-246.2888	20.012	0.250	-246.28838	20.000	0.250	-246.28896	20.036	0.231	-246.28845 ^b	-246.28796
		19.420			19.412			20.000			19.501			

Table IV: Expectation values for the excited state ($1s2s\ 1^3S$) using the function $\Psi_G^{(-)}$ constrained/unconstrained. Results by Accad-Pekeris-Schiff [28], Braun-Schweizer-Herold [29] and Liverts-Barnea [15] (*) included for comparison.

Z	E	$C_{Z,e}^{(1)}$	$C_{Z,e}^{(2)}$	$C_{e,e}/4$	$\langle\delta(\mathbf{r}_1)\rangle$	$\langle\delta(\mathbf{r}_{12})\rangle$	$\langle r_1 \rangle$	$\langle r_1^2 \rangle$	$\langle r_{12} \rangle$	$\langle r_{12}^2 \rangle$	source
3/2	-1.17739	1.5	1.5	0.25	0.54779	0	4.07023	30.48296	7.24355	61.24372	
	-1.17758	1.517	0.982	0.206	0.54595	0	4.16499	32.52315	7.43475	65.31719	
2	-2.17501	2	2	0.25	1.32437	0	2.53536	11.23822	4.41675	22.60109	
	-2.17515	2.019	1.482	0.214	1.32265	0	2.55238	11.49963	4.45021	23.10662	
	-2.17523				1.32036	0	2.55046	11.46432	4.44754	23.04620	[28]
	-2.17523				1.32035	0	2.55047		4.44753		[15]
	-2.17522				1.32028		2.55047	11.46438			[29]
10	-60.66847	10	10	0.25	175.8732	0	0.39261	0.24991	0.66026	0.50081	
	-60.66852	10.036	9.538	0.225	175.8991	0	0.39277	0.25034	0.66058	0.50161	
	-60.66835				175.7860	0	0.39276	0.25027	0.66061	0.50155	[28]
	-60.66865				175.7857	0	0.39276		0.66061		[15]
20	-246.28838	20	20	0.25	1420.1148	0	0.19178	0.059305	0.321414	0.11872	
	-246.28896	20.036	19.501	0.231	1419.6493	0	0.19178	0.059248	0.321362	0.118616	
	-246.28908				1419.1334	0	0.19177		0.32137		[15]

* calculated using the code provided in [15]

It can be shown that the Majorana formula holds for this state

$$E^{(1^3S)} = -\frac{5Z^2}{8} + 0.188141 Z - 0.0507843. \quad (36)$$

It provides accuracy 4 s.d. for $2 \leq Z \leq 10$ and 5 s.d. for $Z \geq 10$! In general, the energies of the excited states ($1s2s\ 2^1S$) and ($1s2s\ 1^3S$) are close to each other, while at $Z \rightarrow \infty$ these states become degenerate, see (10) and (25), respectively.

In Table IV six expectation values for the excited state ($1s2s\ 1^3S$) using the function $\Psi_G^{(-)}$ are presented in the two cases of the constrained function which reproduces the cusp parameters exactly, and unconstrained one. There exists the agreement with results by Accad-Pekeris-Schiff [28], Braun-Schweizer-Herold [29] and [15], wherever possible, in 2-3-4 s.d.

A simple interpolation of the energies obtained with the un-constrained function $\Psi_G^{(-)}$ (see Table III) shows that the critical charge for which the system has a vanishing ionization energy is $Z = Z_{cr} \simeq 1.085$. At this point the function $\Psi_G^{(-)}$ remains square-integrable.

C. Square-integrability of compact functions

As was stated in Section I.D if keeping the position of one electron fixed the wavefunction decays exponentially at large values of the position of another electron, at least for $Z > 1$. It can be seen explicitly if we take the first term in $\Psi^{(-)}(r_1, r_2, r_{12})$ in (20). Similar relations as (15) are obtained for $\phi|_{r_2(r_1)fixed}$. For the exact solution (23) the corresponding parameters $A_{1,2}$ in (15) are,

$$A_1^{(-)} = \frac{1}{2}Z, \quad A_2^{(-)} = Z,$$

they correspond to the Coulomb charges on $2s(1s)$ orbitals. It implies that at $Z = Z_B^{(-)} = 0$ square-integrability of (23) is lost.

Taking the first term in $\Phi_G^{(-)}(r_1, r_2, r_{12})$ in (33) we arrive at the parameters for the lowest spin-triplet excited state (ES3),

$$A_1^{ES3} = \alpha Z \frac{c_1}{d_1} - \gamma \frac{c_{12}}{d_{12}}, \quad A_2^{ES3} = \beta Z - \gamma \frac{c_{12}}{d_{12}}. \quad (37)$$

It turns out that in concrete calculations, for all studied Z ,

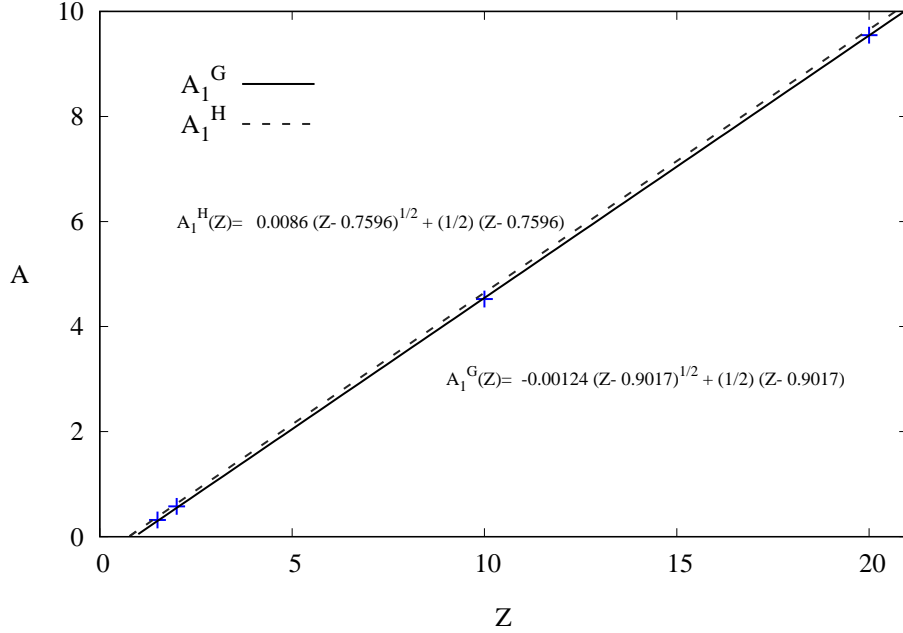
$$A_1^{ES3} < A_2^{ES3},$$

for both functions $\Psi_H^{(-)}$ and $\Psi_G^{(-)}$ as the appearance of clusterization effect. In Fig.6 the behavior of A_1^{ES3} vs Z for functions $\Psi_H^{(-)}$ and $\Psi_G^{(-)}$ is shown. With high accuracy for both functions it is a straight line with slope 1/2. At $Z = Z_B^{(ES3)} \simeq 0.90$ (0.76) it crosses the horizontal line where the function $\Psi_G^{(-)}$ ($\Psi_H^{(-)}$) becomes non-square-integrable. It is natural to assume that the Z -complex plane of energy has the square-root branch point at $Z = Z_B^{(ES3)}$, where the energy level 1^3S crosses with the energy level 2^3S . It seems likely, that in this point the Puiseux expansion in $(Z - Z_B^{(ES3)})$ can be built, cf. [9] and references therein. It will be done elsewhere.

CONCLUSIONS

In this article the few-parametric ultra-compact variational trial functions are constructed for spin-singlet ($1s2s2^1S$) and spin-triplet ($1s2s1^3S$) states for He-like iso-electronic sequence with $Z \in [2, 20]$. In the limit $Z \rightarrow \infty$ these functions become the exact eigenfunctions for the problem of two non-interactive Hydrogen atoms. At $Z \in [2, 20]$ they allow us to

Figure 6: He-like sequence, state ($1s2s\ 1^3S$):
the parameter A_1 vs Z , see text: (37) for the function $\Psi_G^{(-)}$ (33) (with un-constrained parameters) found numerically (marked by crosses) and fitted (solid line) with $Z_B^{(ES3)} \sim 0.902$ compared with $A_1 = (\alpha Z - \gamma)$ for (30) - dashed line, which predicts $Z_B \sim 0.760$; $A_1^{(H,G)}$ “measures” the square-integrability of functions (33) and (30), respectively.



reproduce the energies with 4-5 s.d. and some expectation values with 2-3 s.d. while the cusp parameters are reproduced exactly. We assume that all obtained figures can not be changed by mass, relativistic and QED corrections. With high accuracy these figures are reproduced by the Majorana formula - the second degree polynomial in Z .

In general, the atomic ions with $Z > 2$ are poorly studied and many of our results are presented for the first time. It turned out that the surprising observation by Bressanini-Reynolds about a special form of nodal surface for 2^1S state made for Helium atom can be extended to the atomic ions with $Z > 2$. It is crucial for Monte-Carlo studies of the excited states of highly charged ions. Methodology which we presented can be easily extended for building the ultra-compact functions for other excited states of He-like sequence. It will be done elsewhere.

In the Part III [30] the spin-quartet state 1^40^+ of Li-like sequence will be studied using ultra-compact trial functions for $Z \leq 20$.

ACKNOWLEDGMENTS

J.C. del V. is supported by CONACyT PhD Grant No.570617 (Mexico) and by postdoctoral grant via DGAPA grant IN113819 (Mexico). This work is partially supported by CONACyT grant A1-S-17364 and also DGAPA grant IN113819 (Mexico). D.J.N. is supported in part by PRODEP project 42027 UV-CA-320 (Mexico).

-
- [1] A.V. Turbiner, J.C. López Vieyra, J.C. Valle, D.J. Nader,
Ultra-Compact accurate wave functions for Helium-like and Lithium-like iso-electronic sequences and variational calculus. I. Ground state,
Int Journal of Quantum Chem 2021; 121: qua.26586
doi.org/10.1002/qua.26586
ArXiv: 2007.11745: pp.40, 7 tables (July-November 2020); extended, pp.44 (December 2020)
- [2] F.E. Harris and V.H. Smith Jr.,
J. Phys. Chem. A **109** (2005) 11413-11416
- [3] C.W. David,
Phys. Rev. A **74**, 014501 (2006)
- [4] N.L. Guevara, F.E. Harris and A.V. Turbiner,
Int. Journ. Quant. Chem, **109**, 3036-3040 (2009)
- [5] A.V. Turbiner, J.C. López Vieyra,
The ground state of the H_3^+ molecular ion: physics behind,
invited contribution: Oka-Festschrift
Journal of Physical Chemistry A **117** (2013) 10119 - 10128
- [6] L. Bertini, M. Mella, D. Bressanini, G. Morosi,
J. Phys. **B34**, 257-265 (2001)
- [7] E.A. Hylleraas,
Neue Berechnung der Energie des Heliums im Grundzustande, sowie des tiefsten Terms von Ortho-Helium,
Z. Phys. **54** 347-366 (1929) (in German);
English translation: Quantum chemistry: classic scientific papers, translated and edited by

- H. Hettema, Singapore; London: World Scientific, 2000, pp. 104-121
- [8] R.S. Mulliken,
J. Chem. Phys. **43** S2 (1965)
 - [9] A.V. Turbiner, J.C. López Vieyra, H. Olivares Pílon,
Annals of Physics **409** (2019) 167908 (19 pp)
 - [10] L.U. Ancarani and G. Gasaneo,
J. Phys. B: At. Mol. Opt. Phys. **41** (2008) 105001
 - [11] A. V. Turbiner, W. Miller Jr and M.A. Escobar Ruiz,
Journal of Physics **A50** (2017) 215201;
Journ of Math Physics **A59** (2018) 022108;
Journal of Physics **A51** (2018) 205201;
Journ of Math Physics **A60** (2019) 062101
 - [12] J.E. Gottschalk et al,
J Phys **A20** (1987) 2077-104
 - [13] F. H. Stillinger and D. K. Stillinger,
Phys. Rev. A **10**, 1109 (1974)
 - [14] T. Kinoshita,
Phys. Rev. **105**, 1490-1502 (1957)
 - [15] E.Z. Liverts and N. Barnea,
Comput. Phys. Commun. **182(9)**, 1790-1795 (2011)
 - [16] D. Bressanini, and P. J. Reynolds,
Unexpected Symmetry in the Nodal Structure of the He Atom,
Phys. Rev. Lett. **95**, 110201 (2005);
T.C. Scott et al,
Nodal surfaces of helium atom eigenfunctions,
Phys. Rev. A **95**, 060101(R) (2007)
 - [17] G. W. F. Drake,
in *Springer Handbook of Atomic, Molecular, and Optical Physics*,
(Ed: G.W.F. Drake), Springer New York, New York, Ch. 11, pp. 199-219 (2006)
 - [18] A.V. Turbiner, J.C. López Vieyra, H. Olivares Pílon,
Mod. Phys. Lett. A **31** (2019) 1650156 (10 pp)

- [19] A.V. Turbiner, J.C. López Vieyra,
Can. Jour. Phys. **94**, 249-253 (2016)
- [20] T. Andersen,
Atomic negative ions: structure, dynamics and collisions,
Phys.Repts. **394** (2004) 157–313
- [21] C.S. Estienne, M. Busuttil, A. Moini, and G.W.F. Drake,
Phys. Rev. Lett. **112**, 173001 (2014)
- [22] H. Olivares-Pilon and A.V. Turbiner,
Phys. Lett. A **379**, 688 (2015)
- [23] M. Hoffmann-Ostenhof, Th. Hoffmann-Ostenhof and B. Simon,
J Phys. **A 16** (1983) 1125-1131
- [24] J. Bellazzini et al,
Existence of ground states for negative ions at the binding threshold,
Reviews in Math Phys. **26** (2014) 1350021
- [25] D.P. Chong and D.M. Schrader,
Molecular Physics **16**, 137-144 (1969)
- [26] D.T. Aznabaev, A.K. Bekbaev, and V.I. Korobov,
Phys. Rev. A **98**, 012510 (2018)
- [27] G.W.F. Drake,
Can. Jour. Phys. **66**, 586 (1988)
- [28] Y. Accad, C. L. Pekeris and B. Schiff,
Phys. Rev. A **4**, 516-536 (1971)
- [29] M. Braun, W. Schweizer and H. Herold,
Phys. Rev. A **48**, 1916-1920 (1993)
- [30] D.J. Nader, J.C. Valle, J.C. López Vieyra, A.V. Turbiner,
Ultra-Compact accurate wave functions for He-like and Li-like iso-electronic sequences and variational calculus. III. Spin-quartet state of Lithium sequence
(in preparation)